Deep electrical structure of northern Alberta (Canada): implications for diamond exploration

Erşan Türkoğlu, Martyn Unsworth, and Dinu Pana

Abstract: Geophysical studies of upper mantle structure can provide constraints on diamond formation. Teleseismic and magnetotelluric data can be used in diamond exploration by mapping the depth of the lithosphere–asthenosphere boundary. Studies in the central Slave Craton and at Fort-à-la-Corne have detected conductors in the lithospheric mantle close to, or beneath, diamondiferous kimberlites. Graphite can potentially explain the enhanced conductivity and may imply the presence of diamonds at greater depth. Petrologic arguments suggest that the shallow lithospheric mantle may be too oxidized to contain graphite. Other diamond-bearing regions show no upper mantle conductor suggesting that the correlation with diamondiferous kimberlites is not universal. The Buffalo Head Hills in Alberta host diamondiferous kimberlites in a Proterozoic terrane and may have formed in a subduction zone setting. Long period magnetotelluric data were used to investigate the upper mantle resistivity structure of this region. Magnetotelluric (MT) data were recorded at 23 locations on a north–south profile extending from Fort Vermilion to Utikuma Lake and an east–west profile at 57.2°N. The data were combined with Lithoprobe MT data and inverted to produce a three-dimensional (3-D) resistivity model with the asthenosphere at 180–220 km depth. This model did not contain an upper mantle conductor beneath the Buffalo Head Hills kimberlites. The 3-D inversion exhibited an eastward dipping conductor in the crust beneath the Kiskatinaw terrane that could represent the fossil subduction zone that supplied the carbon for diamond formation. The low resistivity at crustal depths in this structure is likely due to graphite derived from subducted organic material.

Résumé : Des études géophysiques de la structure du manteau supérieur peuvent encadrer notre connaissance de la formation des diamants. Des données télésismiques et magnétotelluriques peuvent être utilisées dans l'exploration pour des diamants en cartographiant la profondeur de la limite lithosphère–asthénosphère. Des études dans le centre du craton des Esclaves et à Fort-à-la-Corne ont révélé des conducteurs dans le manteau lithosphérique à proximité de kimberlites diamantifères ou sous ces dernières. Le graphite peut potentiellement expliquer la conductivité rehaussée et pourrait impliquer la présence de diamants à de plus grandes profondeurs. Des arguments pétrologiques suggèrent que la croûte lithosphérique peu profonde soit trop oxydée pour contenir du graphite. D'autres régions diamantifères ne montrent aucun conducteur dans le manteau supérieur, suggérant que la corrélation avec des kimberlites diamantifères ne soit pas universelle. Les Buffalo Head Hills de l'Alberta contiennent des kimberlites diamantifères dans un terrane datant du Protérozoïque et ces kimberlites peuvent avoir été formées dans un environnement de zone de subduction. Des données magnétotelluriques de longue période ont été utilisées pour étudier la structure de la résistivité du manteau supérieur de cette région. Des données magnétotelluriques ont été enregistrées à 23 emplacements selon un profil nord–sud s'étendant de Fort Vermilion au lac Utikuma et selon un profil est-ouest à une latitude de 57,2° N. Les données ont été combinées aux données magnétotelluriques Lithoprobe et inversées pour produire un modèle de résistivité 3-D avec l'asthénosphère à une profondeur de 180–220 km. Ce modèle ne contenait pas de conducteur du manteau supérieur sous les kimberlites de Buffalo Head Hills. L'inversion 3-D montrait un conducteur à pendage est dans la croûte sous le terrane de Kiskatinaw, qui pourrait représenter la zone fossile de subduction qui a fourni le carbone pour la formation des diamants. La faible résistivité à des profondeurs crustales est sans doute due à du graphite provenant du matériel organique subducté.

[Traduit par la Rédaction]

Introduction

Diamonds are formed in the mantle at depths where the pressure causes carbon to be present as diamond rather than graphite (Boyd and Gurney 1986) and their exposure at the surface is a result of rapid transport to the surface within kimberlitic magmas. Diamonds can be broadly divided into those derived from peridotite and eclogite hosts (Stachel and Harris 2008), and a debate continues about the origin of the carbon found in these diamonds. One view is that the carbon for eclogitic diamonds originates as organic material and carbonates transported to depth in subduction zones (Tappert et al. (2005), while the carbon in peridotitic diamonds is derived from a mantle source (Kirkley et al. 1991). An alternative view suggests that a common primordial source of carbon is responsible for the formation of both eclogitic and peridotitic diamonds with open-system carbon isotopic fractionation involving a CO_2 fluid and leading to isotopically light (non-mantle) values of carbon being

Received 13 August 2008. Accepted 12 February 2009. Published on the NRC Research Press Web site at cjes.nrc.ca on 27 March 2009.

Paper handled by Associate Editor F. Cook.

E. Türkoğlu and M. Unsworth.[1] University of Alberta, Department of Physics, 11322-89 Avenue, Edmonton AB T6G 2G7, Canada.
D. Pana. Alberta Geological Survey, 4th Floor, Twin Atria Building, 4999-98 Avenue, Edmonton, AB T6B 2X3, Canada.

[1]Corresponding author (e-mail: unsworth@phys.ualberta.ca).

restricted to eclogitic diamond sources (Cartigny 2005). In peridotitic source regions, a free CO_2 fluid cannot exist (Wyllie and Huang 1976) and the isotopic signature of primordial carbon is preserved. The majority of diamonds appear to have formed in peridotitic ($\sim$2/3) and the minority in eclogitic ($\sim$1/3) sources within deep lithospheric roots beneath cratons (Stachel and Harris 2008). In some unconventional diamond deposits, including the Slave Craton, a significant fraction of diamonds of eclogitic affinity was formed in the sublithospheric mantle at depths in excess of 600 km (Stachel and Harris 2008).

Ongoing diamond exploration requires analysis of many geological, geochemical, and geophysical parameters. Even with exploration limited to regions of ancient, thick lithosphere, the search for diamond-bearing kimberlites requires very large areas to be covered. Additional criteria for focused exploration are potentially useful. Previous geophysical applications in diamond exploration have focused on shallow-depth studies aimed at locating kimberlite pipes (Power et al. 2004). Deep-sounding geophysical methods can contribute to diamond exploration in two distinct ways.

The primary application of deep geophysical methods in diamond exploration has been to determine the depth of the lithosphere–asthenosphere boundary. This exploits the fact that a significant change in seismic and electrical properties occurs across this interface. In terms of electrical properties, the lithospheric mantle has a resistivity of 100 – 10 000 Ωm and decreases in the asthenosphere due to a number of effects (Xu et al. 2000). Increasing temperature causes thermal activation of charge carriers and allows them to move more easily through mineral lattices. If present, partial melt permits ions to move more easily through the melt phase. Laboratory experiments by Schilling et al. (1997) and Partzsch et al. (2000) showed that 2% partial melting occurs in typical mantle rocks at 1030 °C at atmospheric pressure (1 atm = 101.325 kPa). Partial melting at the lithosphere–asthenosphere boundary can produce a factor of ten decrease in the bulk electrical resistivity that can be detected from the surface with long-period magnetotelluric data. Diffusion of hydrogen ions can also enhance the electrical conductivity of the upper mantle (Karato 1990).

A second way that deep geophysical exploration can potentially be used in diamond exploration is by identifying constraints on upper mantle composition. This approach was suggested by Jones and Craven (2004), who noted that diamondiferous kimberlites of Eocene age in the central Slave Craton are underlain by a prominent upper mantle conductor (Jones et al. 2003). Partial melting at a depth of 100 km in the central Slave Craton was not a possible explanation because the lithosphere is 200 km thick (Jones et al. 2003). Sulphides were not found in mantle xenoliths and thus cannot be used to explain the high conductivity of the upper mantle, and conduction by hydrogen ions is unlikely in Archean lithosphere with a low volatile budget. The explanation preferred by Jones and Craven (2004) for the elevated upper mantle electrical conductivity beneath the central Slave Craton was interconnected graphite films. Jones and Craven (2004) speculated that graphite in the shallow upper mantle could imply that, at greater depths in the diamond stability field, a carbon-rich mantle would contain diamonds. A second example of an upper mantle conductor being observed close to diamondiferous kimberlites was reported by Jones et al. (2005). In this study, a mantle conductor was observed 100 km from the Fort-à-la-Corne kimberlites in Saskatchewan was inferred to extend beneath the surface expression of the kimberlites. However, a correlation of diamonds and an anomalous upper mantle resistivity structure does not appear to be universal. Jurassic kimberlites in the northern Slave Craton and Cambrian kimberlites in the southern Slave Craton are not underlain by upper mantle conductors (Jones et al. 2003). A study of the Kaapvaal craton has shown that no upper mantle conductor is present beneath the type-example of kimberlites (Jones et al. 2006).

The hypothesis that graphite is present above the diamond stability field is not without some petrological problems, as (1) graphite films from these depths have not been observed in xenoliths, and (2) the shallow lithospheric mantle may be too oxidized for carbon to be present as graphite rather than carbonate.

This paper describes an investigation of the mantle structure beneath northern Alberta in the vicinity of recently discovered diamondiferous kimberlite pipes in the Buffalo Head Hills (Fig. 1). The study had two objectives:

(1) to determine whether the upper mantle at this location has anomalous electrical properties that might be associated with the occurrence of diamondiferous kimberlites, and

(2) to extend the previous Lithoprobe studies of the area by Boerner et al. (2000) with a three-dimensional (3-D) approach.

Geological setting

The surface geology in the field area is characterized by 1–2 km of Phanerozoic strata of the Western Canada Sedimentary Basin (WCSB). The basement rocks of northern Alberta are generally Archean in age and were variably reworked during the early Proterozoic. They can be divided into distinct continental slivers accreted to the Rae Terrane at 2.0–1.8 Ga (Ross et al. 1994, Burwash et al. 2000; Chacko et al. 2000; De et al. 2000). The Buffalo Head Terrane, which hosts the Buffalo Head Hills kimberlites, is 200–300 km wide, with no surface exposure of basement rocks, and was defined from characteristic patterns of aeromagnetic anomalies (Fig. 1; Ross et al. 1994; Pilkington et al. 2000). The crust of the Buffalo Head Terrane is of Paleoproterozoic (2.3–2.0 Ga) metamorphic age (Thériault and Ross 1991; Villeneuve et al. 1993), and can be divided into three subdomains on the basis of aeromagnetic anomalies (Ross et al. 1991). It consists primarily of metaplutonic rocks ranging in composition from gabbro to leucogranite (Thériault and Ross 1991; Burwash et al. 2000). The centre of the Buffalo Head Terrane includes the Red Earth granulite domain, characterized by high-grade metamorphic conditions.

The Buffalo Head Hills kimberlite field is late Cretaceous (88–70 Ma) in age (Carlson et al. 1999; Skelton et al. 2003; Eccles et al. 2004). At least 26 of the 38 kimberlite pipes are diamondiferous (Hood and McCandless 2004). Most conventional diamond deposits are found in Archean cratons that have not been subsequently modified by tectonothermal

Fig. 1. Basement geology of the study area after Villeneuve et al. (1993) based on potential field signatures, core samples, and extrapolation to outcrop in the Canadian Shield. Diamonds show kimberlite pipes, small circles show long-period magnetotelluric stations, and dashed lines indicate the major conductivity anomalies in the study area (Boerner et al. 2000). KC, Kiskatinaw conductor; GSLSZ, Great Slave Lake shear zone.

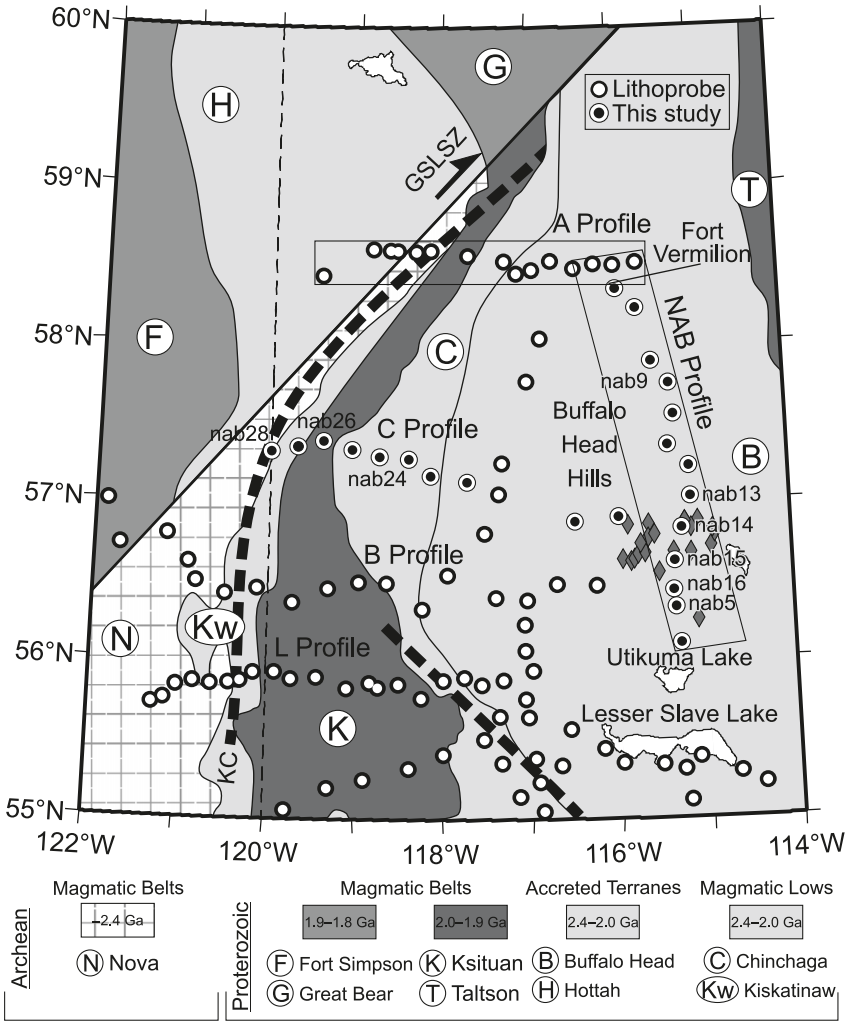

events (Janse 1994). However, diamonds are sometimes found in terranes of Paleoproterozoic age, such as the Buffalo Head Terrane (Banas et al. 2007). Analyses of mantle xenoliths showed an upper mantle with composition dominated by lherzolite and give evidence that potentially pre-existing Archean lithospheric mantle had been strongly overprinted by subsequent tectonothermal and metasomatic events in the Early Proterozoic (Aulbach et al. 2004; Hood and McCandless 2004). Geochronological studies on xenoliths from the K6 pipe indicate the basement was affected by a tectonothermal event around 1940 Ma, similar in timing to an event detected in the Taltson magmatic zone to the east (Eccles et al. 2006). Xenolith studies were used to define a geothermal gradient consistent with a lithospheric thickness of ~180 km (Aulbach et al. 2004). Many of the Buffalo Head Hills diamonds clearly show a conventional lithospheric origin and were formed within peridotitic–eclogitic hosts within the subcontinental lithosphere (Banas et al. 2007). However, a significant proportion (40%–50%) of the diamonds indicate a sublithospheric origin in broadly basaltic bulk compositions, which may reflect diamond formation in a descending slab at asthenospheric depths (300–400 km) (Davies et al. 2004; Banas et al. 2007). The carbon isotope characteristics of some of these sublithospheric eclogitic diamonds is consistent with carbon being derived from organic material transported to depth by a subducting slab (Davies et al. 2004; Banas et al. 2007). It has been suggested that these diamonds were transported from deeper levels to the base of the lithosphere by mantle flow within a plume (Davies et al. 2004).

Previous geophysical studies

Extensive hydrocarbon and mineral exploration has taken place in northern Alberta, but most geological and geophysical data remain in the private domain. Teleseismic studies can be relevant to diamond exploration, but limited data are available in northern Alberta. Studies further south showed that the southern Hearne Province was characterized by high seismic velocities to a depth of 200–250 km, which was interpreted as the base of the lithosphere (Shragge et al. 2002). Regional surface wave analysis showed a litho-

sphere thickness of 180–220 km in northern Alberta (McKenzie and Priestley 2008). Shear wave-splitting revealed polarization directions with a N37°E–N53°E trend, parallel to geologic strike directions in the upper crust (Shragge et al. 2002). Lithoprobe active-source seismic data determined a crustal thickness of 40 km at Peace River (117°W –120°W and 56°N). These data also show east-dipping reflections that have been interpreted as the east-dipping Kiskatinaw–Ksituan boundary along lines 11 and 12 of the PRAISE (Peace River Arch Industry Seismic Experiment) survey (Ross and Eaton 2002). These reflections dip eastward at 25° to a depth of 40 km and are interpreted as the location of subduction and collision events associated with the Proterozoic assembly of Laurentia.

The magnetotelluric (MT) method provides images of subsurface electrical resistivity structure from the surface to mid-mantle depths (Cagniard 1953; Simpson and Bahr 2005). As outlined earlier in the text, resistivity is sensitive to the presence of conducting phases, such as saline fluids, graphite, and partial melt. Since the depth of penetration is controlled by the frequency, exploration to upper mantle depths requires the use of low-frequency (long-period) electromagnetic (EM) signals. Long-period MT data were recorded at 323 sites during the Lithoprobe Alberta Basement Transect (Boerner et al. 2000). The Lithoprobe MT data revealed a number of conductors (Boerner et al. 2000) that included (1) the Kiskatinaw conductor (KC), which follows the Kiskatinaw low-magnetic anomaly in northwest Alberta and northeastern British Columbia; (2) the Red Deer conductor (RDC) in central Alberta, which is approximately coincident with a magnetic anomaly along the Snowbird Tectonic Zone (STZ); and (3) a crustal conductivity anomaly that was identified southwest of Lesser Slave Lake. The first two of these crustal conductors are associated with inferred ancient suture zones (Ross et al. 1994), and the high conductivity is believed to be a consequence of graphite concentration at crustal depths.

Boerner et al. (1999) analyzed MT data collected across the Archean Churchill Province (ACP) and the Snowbird Tectonic Zone, and showed that the upper mantle beneath the Archean terranes was apparently more conductive than the upper mantle beneath the Paleoproterozoic crustal rocks by one order of magnitude. This increase in conductivity was interpreted by Boerner et al. (1999) as a result of extensive metasomatism that occurred during subduction. However, subsequent studies have shown that metasomatism does not always decrease upper mantle resistivity. Jones et al. (2002*b*) showed that a section of the Snowbird Tectonic Zone adjacent to Hudson Bay that has undergone metasomatism was actually highly resistive.

The discovery of the Buffalo Head Hills kimberlites occurred after the Lithoprobe work in Alberta. As a consequence, the MT station distribution was not ideal for imaging the lithosphere beneath the kimberlites. Additional MT data were required to study the location of the kimberlites in terms of crustal and mantle resistivity structure.

Magnetotelluric data collection

Long-period MT data were collected in northern Alberta in 2004 at thirteen locations along a profile from Utikuma Lake to Fort Vermilion (Fig. 1). An additional ten MT stations were deployed along the Chinchaga Forestry Road in 2006. The station distribution was designed to image upper mantle structure beneath the Buffalo Head Hills kimberlites. Magnetotelluric data were recorded at each station for one month with a sample rate of 8 Hz using a NIMS (Narod Intelligent Magnetotelluric System) instrument. Two orthogonal electric field and three magnetic field components were recorded as a function of time. The timing of each instrument was synchronized using signals from global positioning system (GPS) satellites. All MT stations were placed at least 500 m away from pipelines to minimize the effects of noise arising from cathodic protection.

Magnetotelluric data analysis

Dimensionality

The dimensionality of MT data is important since it determines the approach that should be used for interpretation. The skew can be used to qualitatively identify 3-D effects in MT data, although quantitative approaches with a specific threshold for 3-D behavior must be used with caution if the data are noisy (Swift 1967; Bahr 1988). Figure 2 shows the Bahr skew values in pseudosection format. Since depth of penetration increases with signal period, this type of display gives an impression of depth on the vertical scale. The NAB (northern Alberta) magnetotelluric profile appears to be relatively two-dimensional (2-D), while the west ends of the L and A profiles show strong indications of 3-D effects at periods in the range 10–1000 s. Note that there is a smooth variation in skew values from site-to-site, showing that noise is not the cause of high skew values.

Geoelectric strike direction

The 2004–2006 MT data were combined with Lithoprobe data, and the geoelectric strike directions were computed with the tensor decomposition algorithm of McNeice and Jones (2001). The MT strike direction computed with tensor decomposition has an inherent 90° ambiguity, as shown in Fig. 3. The absolute strike cannot be determined using the MT data alone; other information such as the local geology or induction vectors can be used to overcome this ambiguity. Overall the strike directions are consistent from site-to-site at each period with a direction in the range NNE to NE (or alternatively ESE to SE). At periods longer than 320 s, some stations west of 118°W longitude and south of 58°N latitude show N0°E strike direction. Tensor decomposition gave generally low misfit values, indicating that the data were relatively 2-D in a more objective way than using skew values.

A geoelectric strike direction of N37°E was chosen for initial 2-D analysis of the MT data (Fig. 3). This direction was preferred to N127°E because it was closer to the dominant strike of the geological terranes and the major shear zones (Fig. 1). Note that there is not an exact correspondence between the strike direction derived from tensor decomposition and the fabric of the regional geology. Similar geoelectric directions were observed in the SNORCLE (Slave – Northern Cordillera Lithospheric Evolution Project) survey in northern Canada (Wu et al. 2005). It can also be shown that the choice of a N37°E strike direction is also supported by

Fig. 2. Bahr skew values for NAB, A, and L profiles in pseudosection format.

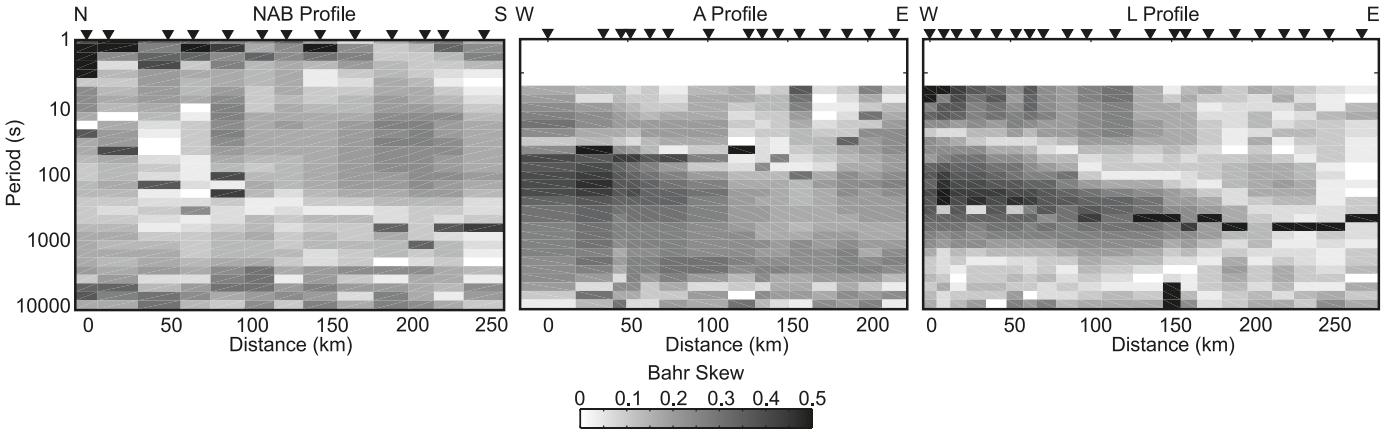

the 3-D inversion model. The dimensionality of the Lithoprobe MT data was described by Jones et al. (2002*a*), who showed that most of the Alberta basement MT data could be considered one dimensional (1-D) at short periods (up to 4 s) representing the sedimentary rocks of the WCSB. For intermediate periods (4–1280 s), some stations were classified either as 2-D or 3-D. At longer periods, Jones et al. (2002*b*) showed a response that could be due to a 2-D mantle structure combined with a 3-D or anisotropic crustal structure.

The ratio of vertical to horizontal magnetic field variations at an MT station is called the tipper (Vozoff 1991). Tipper data can be used to study the dimensionality of the subsurface resistivity and can be plotted as real and imaginary induction vectors. Depending on the convention used, the real component either points away from conductors (Wiese 1962) or towards conductors (Parkinson 1959). The amplitude and direction of these vectors can be affected by electrical anisotropy (Heise and Pous 2001). Real induction vectors are shown in Fig. 4 in the Wiese convention. At short periods ($\sim$30 s), they are small with a length <0.05 indicating that the shallow resistivity structure is relatively uniform. At intermediate periods (300 s), they show an easterly trend that implies north–south oriented structures. At the longest periods (3000 s), the magnitude of the induction vectors becomes very large (>0.4) and they consistently point northeast. This may be due to the proximity of the survey area to the auroral zone. These electromagnetic signals do not satisfy the plane wave assumptions made in conventional MT data analysis and must be used with caution (Jones and Spratt 2002).

Apparent resistivity and phase curves

If a 2-D analysis is valid, the MT data can be divided into two independent modes. The transverse electric (TE) mode uses electric currents that flow parallel to the strike direction, while the transverse magnetic (TM) mode has electric current flow perpendicular to strike. The apparent resistivity curves for both TE and TM modes on the NAB profile showed smooth variations from site-to-site, indicating that the data were not spatially aliased. The MT curves east of 118°W in Fig. 5 (top row) show an increase in apparent resistivity for both TE and TM modes over the period range 1–300 s. This is caused by the increase in resistivity that occurs as MT signals sample first the low resistivity sedimentary rocks of the WCSB and then the higher resistivity crystalline basement rocks. At signal periods longer than $\sim$300 s, the apparent resistivity curves of both modes decrease for all the stations indicating the presence of an extensive conductor beneath the resistive lithosphere.

Stations west of 118°W longitude exhibit a similar behavior, with the exception of the TE mode in the period range 30–300 s. The minimum in the TE mode apparent resistivity is due to the presence of a shallow conductor. This effect is quite strong and it could be considered analogous to galvanic distortion. However, both 2-D and 3-D inversions were able to give an acceptable qualitative fit to the data, and these data were retained in the analysis. This response was observed in both the Lithoprobe and University of Alberta data. The lack of a response in the TM mode is as expected for a thin conductor oriented along strike. The behavior west of 118°W was attributed by Boerner et al. (2000) to electrical anisotropy.

Figure 6*a* shows the NAB profile as a pseudosection, where increasing period on the vertical scale corresponds to increasing depth of signal penetration. It can be seen that the MT data change smoothly along the profile and that the short period data (1–10 s) exhibit a relatively low apparent resistivity (30 Ωm) along the entire profile in both TE and TM modes, corresponding to low resistivity sedimentary rocks. Longer period data (10–1000 s) sample higher resistivities of the crystalline basement rocks, while the longest periods show low resistivity at great depth, likely corresponding to sublithospheric structures.

Two-dimensional MT inversions

Data collected on the NAB and Lithoprobe profiles show a number of indications that they are 2-D. Therefore, the MT data from these profiles were rotated to a common strike direction (N37°E) and projected onto transects normal to this direction. The MT data were inverted using the 2-D inversion algorithm of Rodi and Mackie (2001). Details of the 2-D inversion are listed in Appendix A. The 2-D inversions for the NAB and A profiles are summarized in Fig. 7, and the fit to the measured MT data is shown in Fig. 5 and Fig. 6. Note that an upper mantle conductor is observed at the north end of the NAB profile. Three-dimensional induction effects can cause 2-D inversions to be invalid, so a 3-D

Fig. 3. Geoelectric strike directions for magnetotelluric data in northern Alberta at periods of 43 s, 160 s, 320 s, and 630 s. Crosses show the direction of two possible strike directions due to the 90° ambiguity in MT strike direction. Basemap symbols the same as for Fig. 1.

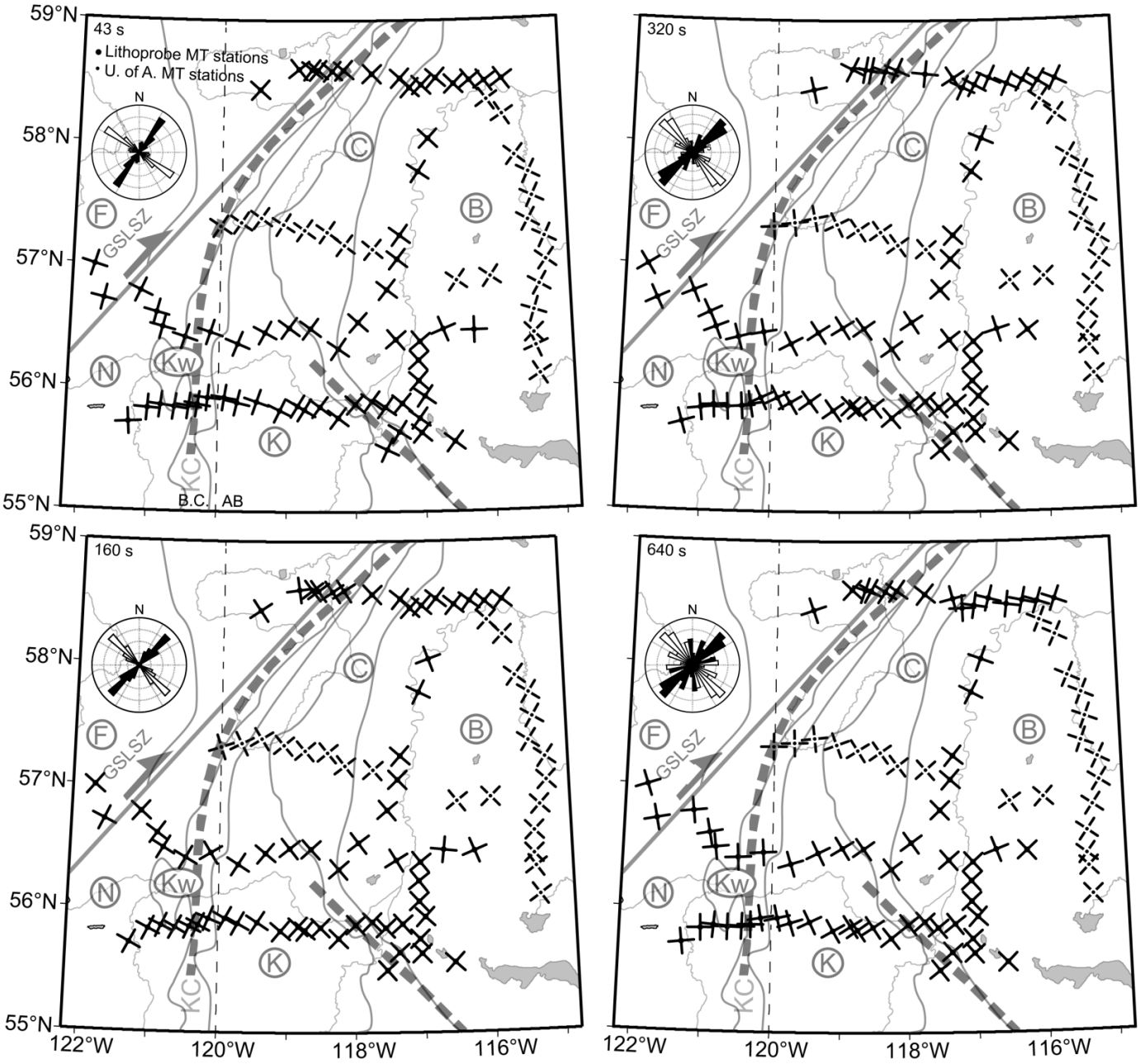

inversion was used to validate the 2-D analysis of the northern Alberta MT data.

Three-dimensional MT inversions

The data were inverted using the 3-D MT inversion algorithm of Siripunvaraporn et al. (2005). A 3-D MT inversion is more demanding than a 2-D MT inversion in terms of computer time and memory requirements. This resulted in the 3-D inversion having less cells in the vertical and horizontal directions than the 2-D inversions. Thus the 3-D inversion models appear blockier than those obtained from 2-D inversions. To implement a 3-D inversion, it was necessary to reduce the number of stations by selecting one from each group of closely spaced stations. The 3-D inversion used the full magnetotelluric impedance tensor with an error floor of 10%. An initial rms (root mean square) misfit of 3.7 was reduced to 1.1 after six iterations to produce the resistivity model shown in Figs. 7 and 8. The starting model included a conductor below 200 km that represented the asthenosphere. The fit to the measured MT data is shown in Fig. 5, and it can be seen that at these representative sites, the 2-D and 3-D inversion give a similar quality fit to the measured MT data.

Figure 7 shows that the 2-D and 3-D inversion models have some similarities. Both show a shallow conductor (WCSB) from 0–10 km and a deep conductor at 200 km that is interpreted as the asthenosphere. On the A profile, a conductor is imaged at mid-crustal depths by both 2-D and

Fig. 4. Real induction vectors plotted using Wiese convention. (*a*) Measured data at periods of 30 s, 300 s, and 3000 s. (*b*) Induction vectors computed from 3-D model presented in Figs. 7 and 8 for the same periods. Basemap symbols the same as for Fig. 1.

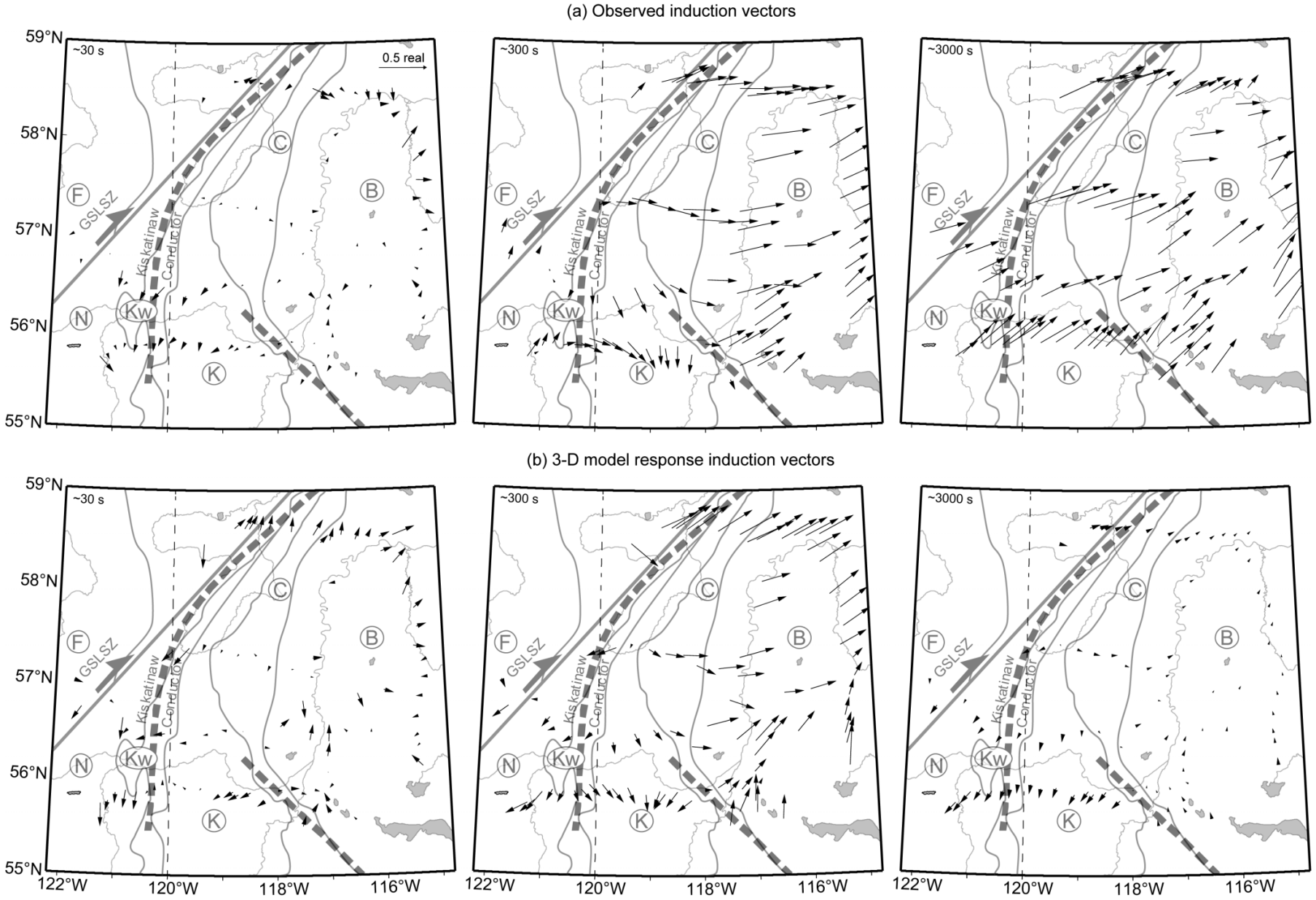

Fig. 5. Apparent resistivity and phase curves representing general characteristics of observed data east of 118°W longitude (top) and west of 118°W longitude (bottom). See Fig. 1 for station locations. Data are displayed in a N37°E coordinate system. Black line shows the fit of the 2-D inversion (Fig. 7). Grey line shows the fit of the 3-D inversion (Figs. 8, 9). Error bars show error floor used in the inversion.

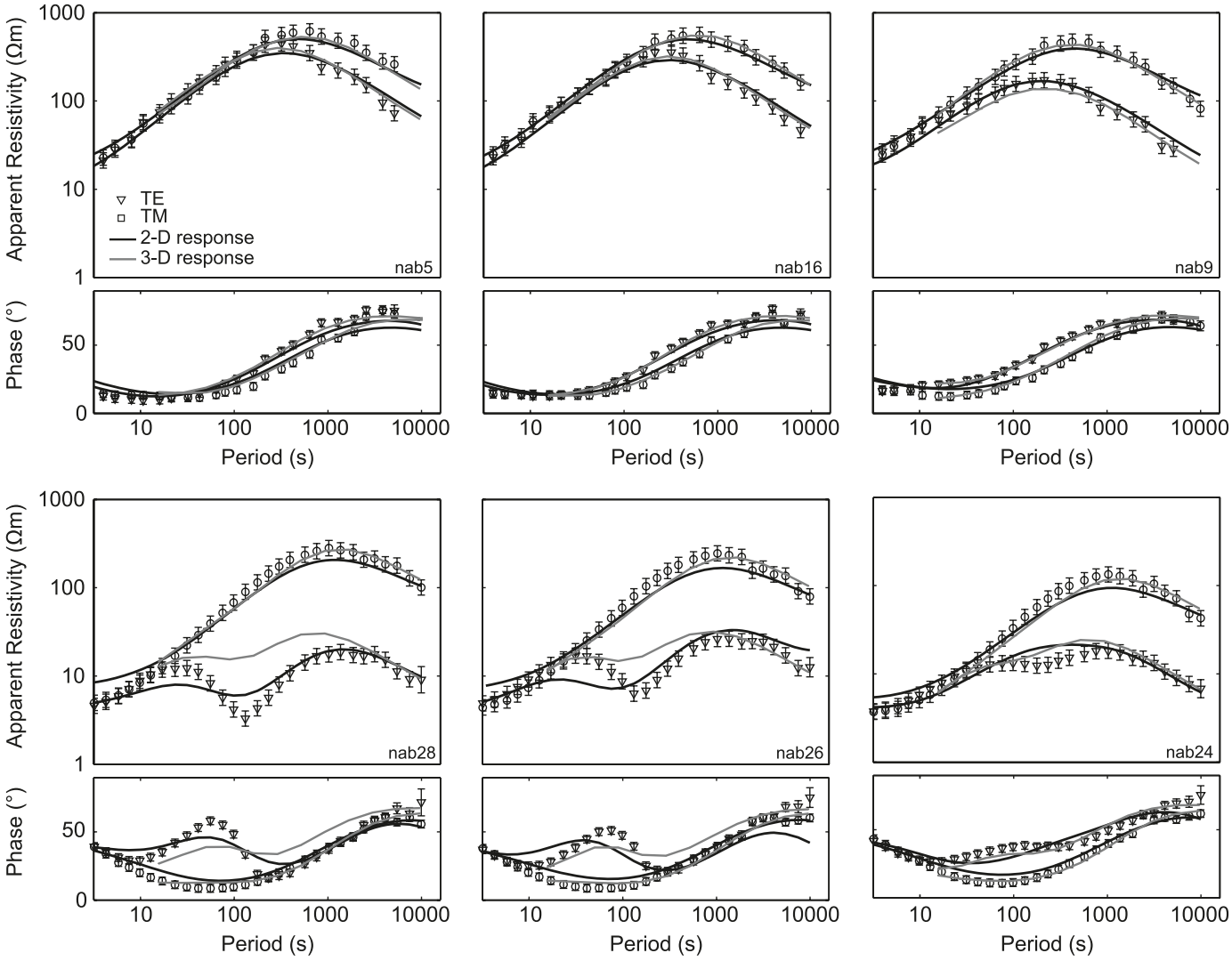

3-D inversions, although the geometry is different. The 3-D inversion shows that this eastward-dipping structure strikes N30°E, parallel to the boundary between Kiskatinaw and Ksituan domains (Fig. 1, Fig. 8). This feature is the Kiskatinaw conductor, which was identified in previous Lithoprobe analyses and which crosses A, B, and L profiles with azimuths of N45°E to N53°E (Boerner et al. 2000). The shallowest part of this anomaly is observed in the southwest corner of the study area (west of L profile) and dips eastward 20° (Fig. 8). This geometry is comparable to the 25° eastward dip angle of prominent seismic reflectors in this location (Ross and Eaton 2002). The depth to the base of a conductor is not well constrained by MT data, but the feature may extend to the Moho. Another related conductivity anomaly is also imaged as a N40°W-striking structure that follows the boundary between the Ksituan and Chinchaga domains. This structure may be part of Kiskatinaw Conductor as imaged in the 3-D inversions, but becomes separate at the latitude of the L profile and further south (Fig. 8). This structure is both smaller and deeper than the main Kiskatinaw Conductor.

However, the 2-D and 3-D inversion models show some important differences. The most significant difference is that the 3-D inversion does not generate the upper mantle conductor beneath the northern part of the NAB profile that was prominent in the 2-D inversion. This feature could be the result of the 3-D effect in MT data being incorrectly interpreted by the 2-D inversions, as further discussed in Appendix A. Note that the conductor beneath the northern NAB profile is due to relatively low apparent resistivities at the northern four stations on the profile. The 2-D inversions that excluded these stations did not generate a conductor.

Source effects in induction vectors

The northern Alberta data show long-period induction vectors with an unusually high amplitude. They could be due to the effect of a distant northwest-striking conductor. One possible location for such a conductor is beneath the Canadian Cordillera, where a conductive crust and shallow asthenosphere are present (Jones and Gough 1995; Soyer and Unsworth 2006). However, 3-D forward modeling stud-

Fig. 6. (*a*) Pseudosection of NAB profile and (*b*) corresponding responses of the 2-D inversion model shown in Fig. 7*a*. ρ and Φ are the apparent resistivity and phase, respectively, of the MT data.

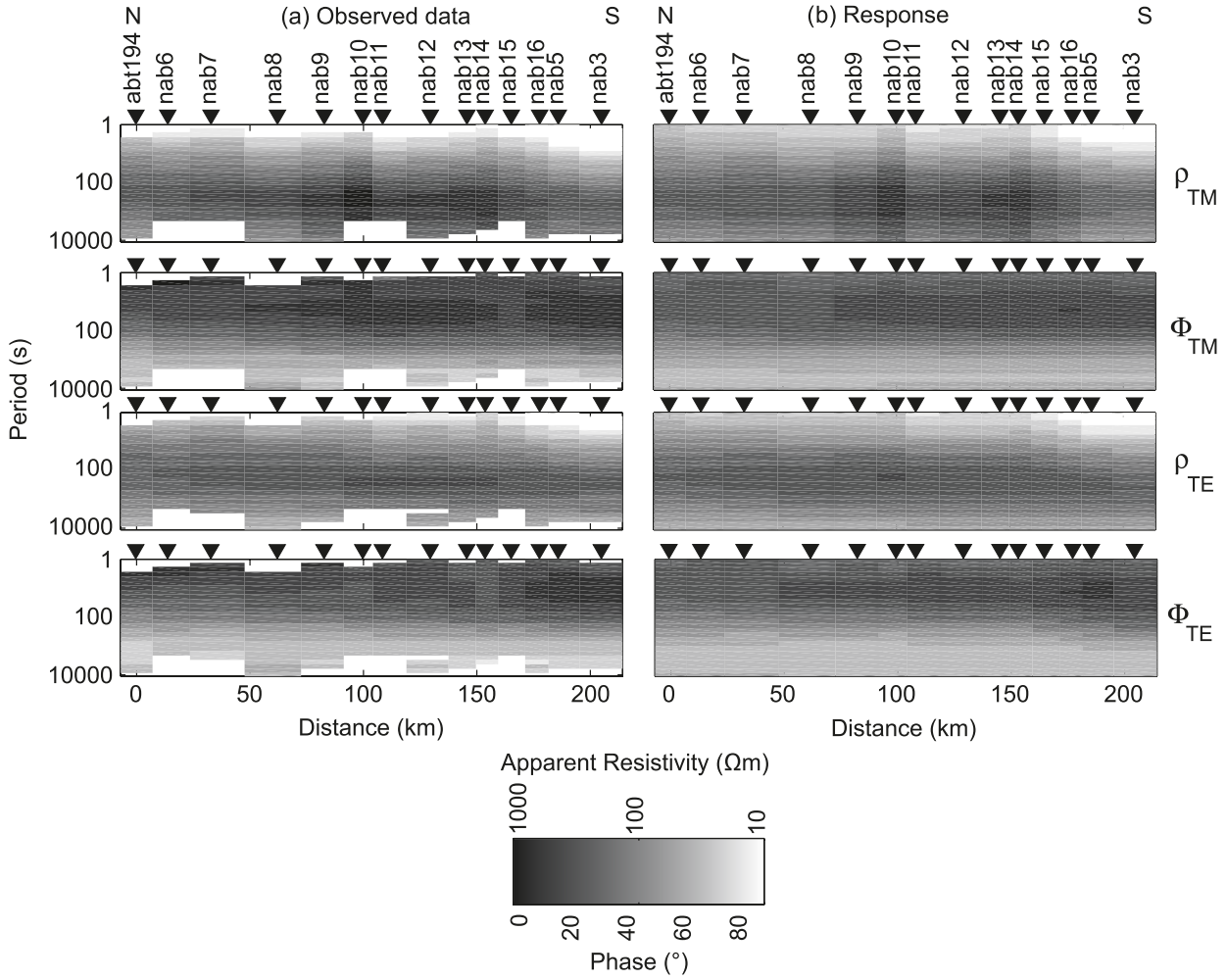

ies showed that it is not possible to produce the observed induction vectors at long periods with a conductor at this, or any other, location.

Given the high magnetic latitude, it is equally possible that the induction vectors are due to non-plane wave effects in the MT signals. The 3-D inversion model was derived from the apparent resistivity and phase data and did not use the induction vectors. The origin of the large induction vectors was investigated by computing the predicted induction vectors for the 3-D model (lower row in Fig. 4). At short periods, the predicted and measured induction vectors are relatively consistent. However, at periods longer than 300 s, the predicted vectors are smaller than the measured vectors. The weak induction vectors predicted by the 3-D model are consistent with the fact that these signals are penetrating to depths of 100–200 km and sampling a layered model comprising resistive lithosphere and conductive asthenosphere. Additional evidence for the induction vectors being due to source effects comes from the fact that the largest amplitudes are observed at the eastern stations, which are closest to the auroral zone. The strong induction vectors measured in northern Alberta are likely due to non-plane wave effects. Note that source effects are generally stronger in the tipper than in the apparent resistivity and phase data (Jones and Spratt 2002).

Discussion

Constraints on depth of the lithosphere–asthenosphere boundary

Lithospheric thickness is an important constraint in diamond exploration. Two approaches were used to determine the depth of the lithosphere–asthenosphere boundary (LAB) in northern Alberta. In the first, a set of constrained 2-D inversions was used. For each inversion, the starting model had a 1000 Ωm lithosphere and a 10 Ωm asthenosphere, and 100 iterations were performed. The asthenosphere resistivity was based on a number of studies including those of Jones and Craven (2004). The inversion used TE and TM mode data at 11 stations at the southern end of the profile. The northern stations on the NAB profile were excluded because of the 3-D effects described earlier. The final rms data misfit shows a broad minimum, with a preferred LAB depth of 200–250 km in northern Alberta. This is in agreement with the LAB depth observed in the unconstrained inversion in Fig. 7. An alternative approach used a 1-D inversion of the invariant (average of the TE and TM modes) at stations closest to the Buffalo Head Hills kimberlites. This gave a consistent LAB depth of 180–220 km (Fig. 9).

Surface wave tomography gives a lithospheric thickness

Fig. 7. Comparison of 2-D and 3-D inversions for the NAB profile and A profile. The northernmost station on the NAB profile is **abt194** from the Lithoprobe magnetotelluric data. rms, root mean square.

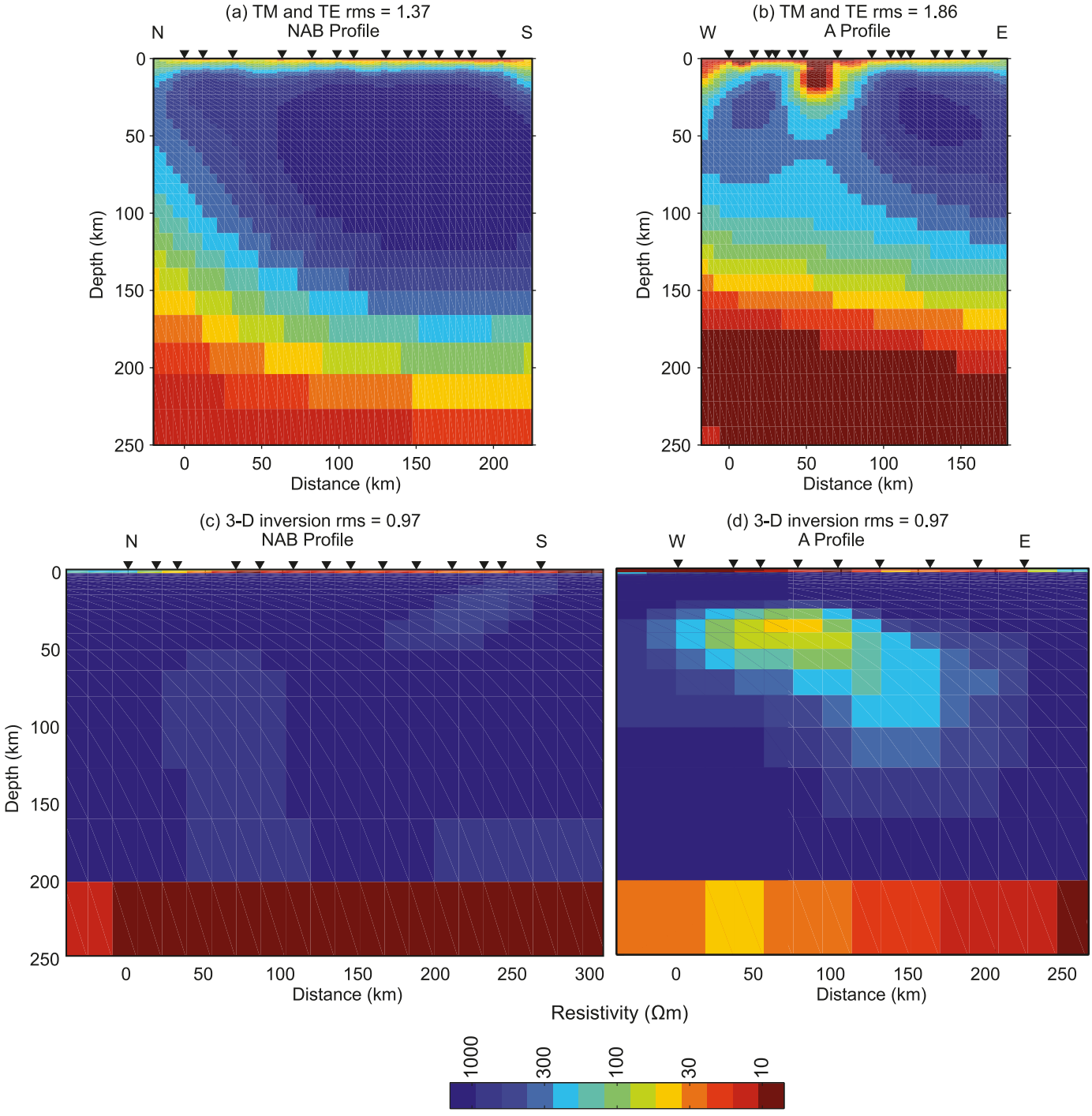

of 180–220 km in northern Alberta (McKenzie and Priestley 2008) . Xenolith studies can also give estimates of LAB depth, typically with a 15 km uncertainty. Thus the 180 km depth derived from geochemical studies of xenoliths (Aulbach et al. 2004) is consistent with the seismic estimate in the Buffalo Head Hills. MT estimates for the LAB are thus consistent with those obtained from mantle xenoliths and seismic studies.

This depth can also be compared with the value of 200 km determined with MT in the central Slave Craton (Jones et al. 2003). In the southern Slave Craton MT gave a depth of 260 km, and petrology suggested 235 ± 15 km (Kopylova and Caro 2004). Seismic thickness was 180–220 km (McKenzie and Priestley 2008), but it should be noted that this was the average value for large region that included both the Slave Craton and surrounding regions.

Structure of an ancient subduction zone

The east-dipping conductor in northern Alberta that was first described by Boerner at al. (2000) is better resolved in

Fig. 8. 3- D resistivity model of lithosphere beneath northern Alberta. Diamonds show the kimberlite pipes and solid black lines outline basement terranes. GSLSZ, Great Slave Lake shear zone.

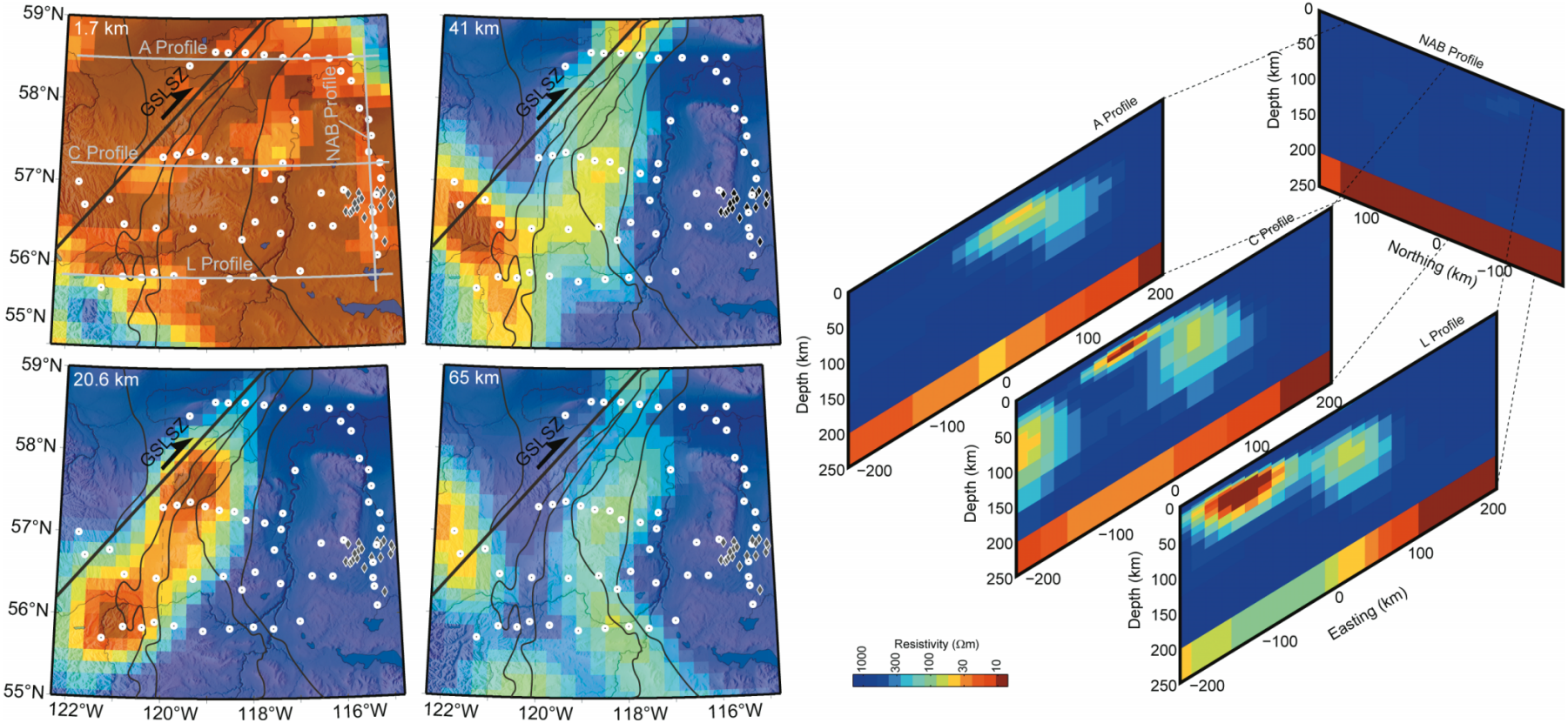

Fig. 9. Upper panel shows normalized r.m.s. (root mean square) data misfit as a function of asthenosphere depth for a set of constrained 1-D inversions for stations on the NAB profile adjacent to the Buffalo Head Hills kimberlites. In each inversion the asthenosphere was fixed, and only resistivity structure above that depth was allowed to change. Lower panel shows the fit to measured data at station nab16.

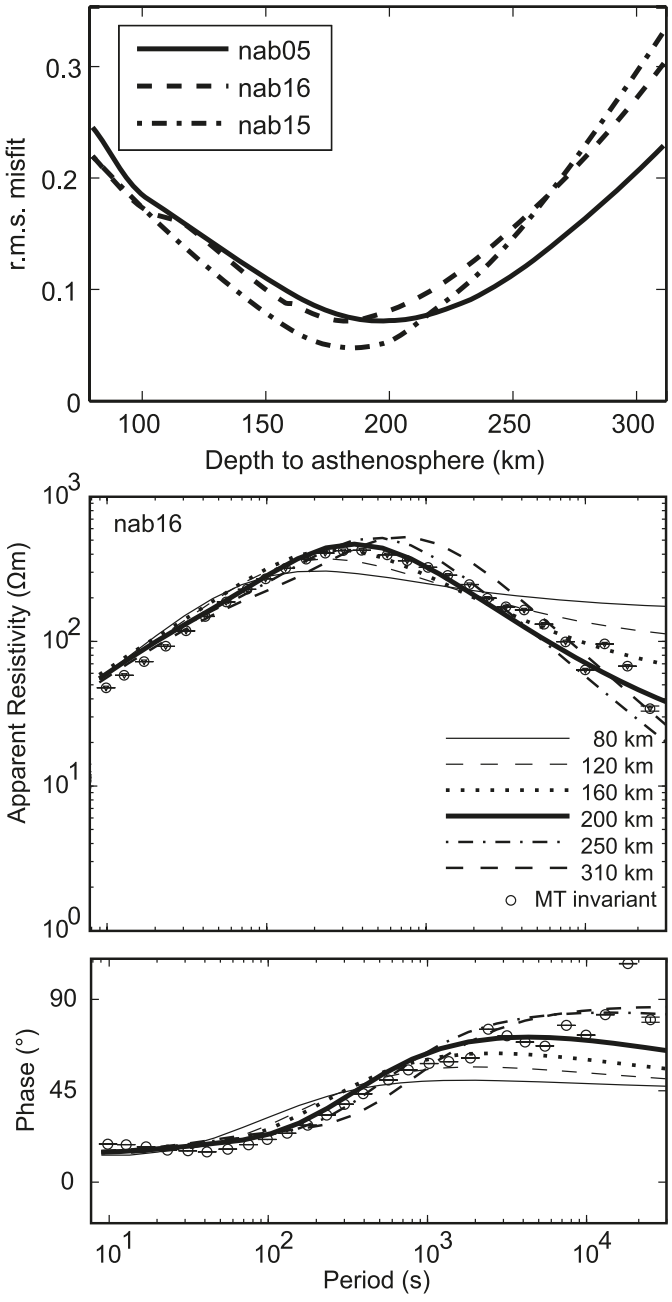

the present study with the collection of additional MT data and use of a 3-D MT inversion algorithm. The top of this feature can be traced from 20 km in the west and to a depth of 50 km in the east. Combined with seismic data and a surface suture zone, this feature can be identified as a fossil subduction zone that dates from the Proterozoic when terrane accretion led to the assembly of this part of Laurentia. Dipping conductors have been observed in a number of other ancient subduction zones including Namibia (Ritter et al. 2005); Fennoscandia (Rasmussen et al. 1987); the Iapetus suture zone (Rao et al. 2007; Tauber et al. 2003); Trans-Hudson Orogen (Jones et al. 2005), and elsewhere in Alberta (Boerner et al. 1995).

Different mechanisms could cause the observed low resistivity, including the presence of sulphides or hydrous minerals (Boerner et al. 2000). However, given the tectonic setting, the low resistivity is likely to be carbon that originated as organic material and carbonates that were transported to depth in an ancient subduction zone and converted into graphite (Jones 1993; Boerner et al. 2000). The presence of a conducting fossil subduction zone could be considered significant for diamond exploration. The high conductivity remaining in the suture suggests that a significant volume of biogenic material was subducted when this feature was active. This in turn implies that carbon was available at lithospheric and sublithospheric depths where the diamonds were formed. The dipping conductor on the C profile has a conductance of 1000–2000 S, which is comparable in magnitude to other conductors observed in fossil subduction zones (Jones 1993), which could indicate that a similar amount of carbon-bearing material was subducted.

These observations are relevant to diamond formation in both the lithosphere and sublithosphere. In a lithospheric environment, this is especially significant for diamond formation in eclogitic source rocks, since it is possible for the carbon to migrate upwards as a mobile CO_2-rich fluid through olivine-free eclogitic lithologies (Luth 1993). Extrapolating the dipping Kiskatinaw conductor east would place the slab at sublithospheric depths beneath the Buffalo Head Hills kimberlites. The fact that the dipping conductor does not extend into the upper mantle could be explained by a number of mechanisms, including changes in oxidation state, lack of interconnection of graphite films with increasing depth, or a decrease in the concentration of graphite.

Conclusions

This study has presented the first 3-D resistivity model for northern Alberta using long-period MT data. Previous MT studies in northern Alberta considered only crustal structure (Boerner et al. 2000). The addition of new MT data has permitted a 3-D interpretation of this area and an investigation to upper mantle depths. The 3-D inversions show no evidence for a zone of enhanced conductivity in the lithospheric upper mantle beneath the Buffalo Head Hills kimberlites. An upper mantle conductor was imaged in the 2-D inversions, but numerical studies showed that this anomaly could be explained as an artifact of the 2-D inversion. The potentially misleading models obtained from 2-D inversions suggest that caution should be used when inverting MT data that give indications that they are 2-D. Even if there are strong indications that MT data can be considered 2-D, a 3-D analysis may be needed to validate this.

The absence of a conductor in the lithospheric upper mantle beneath the Buffalo Head Hills kimberlites gives additional evidence that a spatial correlation between upper mantle conductors and diamondiferous kimberlites is not a universal phenomenon. This lack of correlation appears to be the case for both lithospheric and sublithospheric diamonds and might indicate that the presence of graphite

above the diamond stability field is not always associated with diamond formation below this depth. This could arise through a range of tectonic processes including the suggestion of Helmstaedt and Schultze (1989) that the lower part of cratonic lithosphere was formed from a set of imbricated slices of subducted slab. Unless portions of slab always remain in the graphite stability zone, this process would not produce an upper mantle conductor. Alternatively, if diamonds were formed by mantle metasomatism within eclogite, then the presence of graphite is not required above the zone of diamond formation unless fluids circulated at shallower depths and deposited carbon as graphite. The generally much more depleted character of shallow subcratonic lithospheric mantle (Griffin et al. 1999; Bernstein et al. 2007) suggests that the effects of mantle metasomatism are much more prominent in the deep lithosphere (Stachel et al. 2003). Note that metasomatism can lead to an increase in crustal and upper mantle resistivity (Jones et al. 2002*a*).

In summary, this study has shown how long-period MT data can contribute to studies of diamond formation. The long-period MT data are effective at mapping the depth of the lithosphere–asthenosphere boundary and can also permit the identification of fossil subduction zones that transported carbon to depth. This may be a useful indicator in the exploration for diamonds originating in a subduction zone setting.

Acknowledgments

The authors are grateful to Wolfgang Soyer, Roger Paulen, Andrea Cochrane, Eylem Türkoğlu, Volkan Tuncer, and Edward Bertrand for assistance with magnetotelluric data collection. Funding for this research was provided by the Alberta Ingenuity Fund, Natural Sciences and Engineering Research Council of Canada (NSERC), Canadian Foundation for Innovation, Innovation and Science Research Investments Program (University of Alberta: ISRIP), and the Alberta Geological Survey. Computation was made possible by the use of WestGrid computing resources. Maps were prepared using Generic Mapping Tools of Paul Wessel and Walter H. F. Smith. Alan Jones and Gary McNeice are thanked for making their tensor decomposition software available. Reviews by Alan Jones, Ian Ferguson, and two anonymous reviewers, as well as Associate Editor Fred Cook improved this paper. The authors acknowledge useful discussions with Thomas Stachel.

References

Aulbach, A., Griffin, W.L., O'Reilly, S.Y., and McCandless, T.E. 2004. Genesis and evolution of the lithospheric mantle beneath the Buffalo Head Terrane, Alberta (Canada). Lithos, **77**: 413–451. doi:10.1016/j.lithos.2004.04.020.

Bahr, K. 1988. Interpretation of the magnetotelluric impedance tensor: regional induction and local telluric distortion. Journal of Geophysics, **62**: 118–127.

Banas, A., Stachel, T., Muehlenbachs, K., and McCandless, T.E. 2007. Diamonds from the Buffalo Head Hills, Alberta: Formation in a non-conventional setting. Lithos, **93**: 199–213. doi:10.1016/j.lithos.2006.07.001.

Berdichevsky, M.N., Dmitriev, V.I., and Pzdnjakova, E.E. 1998. On two-dimensional interpretation of magnetotelluric soundings. Geophysical Journal International, **133**: 585–606. doi:10.1046/j.1365-246X.1998.01333.x.

Bernstein, S., Kelemen, P.B., and Hanghoj, K. 2007. Consistent olivine Mg# in cratonic mantle reflects Archean mantle melting to the exhaustion of orthopyroxene. Geology, **35**: 459–462. doi:10.1130/G23336A.1.

Boerner, D.E., Kurtz, R.D., Craven, J.A., Rondenay, S., and Qian, W. 1995. Buried Proterozoic foredeep under the Western Canada Sedimentary Basin? Geology, **23**: 297–300. doi:10.1130/0091-7613(1995)023<0297:BPFUTW>2.3.CO;2.

Boerner, D.E., Kurtz, R.D., Craven, J.A., Ross, G.M., Jones, F.W., and Davis, W.J. 1999. Electrical conductivity in the Precambrian lithosphere of Western Canada. Science, **283**: 668–670. doi:10.1126/science.283.5402.668.

Boerner, D.E., Kurtz, R.D., Craven, J.A., Ross, G.M., and Jones, F.W. 2000. A synthesis of EM studies in the Lithoprobe Alberta Basement Transect: constraints on Paleoproterozoic indentation tectonics. Canadian Journal of Earth Sciences, **37**: 1509–1534. doi:10.1139/cjes-37-11-1509.

Boyd, F.R., and Gurney, J.J. 1986. Diamonds and the African lithosphere. Science, **232**: 472–477. doi:10.1126/science.232.4749.472.

Burwash, R.A., Krupicka, J., and Wijbrans, J.R. 2000. Metamorphic evolution of the Precambrian basement of Alberta. Canadian Mineralogist, **38**: 423–434. doi:10.2113/gscanmin.38.2.423.

Cagniard, L. 1953. Basic theory of the magnetotelluric method of geophysical prospecting. Geophysics, **18**: 605–635. doi:10.1190/1.1437915.

Carlson, S.M., Hillier, W.D., Hood, C.T., Pryde, R.P., and Skelton, D.N. 1999. The Buffalo Head Hills kimberlites: a newly discovered diamondiferous kimberlite province, north-central Alberta, Canada. *In* 7th International Kimberlite Conference, Proceedings: The J.B. Dawson Vol., Cape Town, South Africa. pp. 109–116.

Cartigny, P. 2005. Stable isotopes and the origin of diamond. Elements, **1**: 79–84. doi:10.2113/gselements.1.2.79.

Chacko, T., De, K.S., Creaser, R.A., and Muehlenbachs, K. 2000. Tectonic setting of the Taltson magmatic zone at 1.9–2.0 Ga: a granitoid-based perspective. Canadian Journal of Earth Sciences, **37**: 1597–1609. doi:10.1139/cjes-37-11-1597.

Davies, R.M., Griffin, W.L., O'Reilly, S.Y., and McCandless, T.E. 2004. Inclusions in diamonds from the K14 and K10 kimberlites, Buffalo Hills, Alberta, Canada: diamond growth in a plume? Lithos, **77**: 99–111. doi:10.1016/j.lithos.2004.04.008.

De, K.S., Chacko, T., Creaser, R.A., and Muehlenbachs, K. 2000. Geochemical and Nd–Pb–O isotope systematics of granites from the Taltson Magmatic Zone, northeast Alberta: implications for early Proterozoic tectonics in western Laurentia. Precambrian Research, **102**: 221–249. doi:10.1016/S0301-9268(00)00068-1.

Eccles, D.R., Heaman, L.M., Luth, R.W., and Creaser, R.A. 2004. Petrogenesis of the northern Alberta kimberlite province. Lithos, **76**: 435–459. doi:10.1016/j.lithos.2004.03.046.

Eccles, D.R., Payne, J.G., Simonetti, A., and Hood, C.T.S. 2006. Petrography and geochronology of crustal xenoliths from northern Alberta kimberlite. Alberta Energy and Utilities Board, EUB/AGS Geo-Note 01, 24 p.

Griffin, W.L., Doyle, B.J., Ryan, C.G., Pearson, N.J., Davies, R., Kivi, K., Achterbergh, E.V., and Natapov, L.M. 1999. Layered mantle lithosphere in the Lac de Gras area, Slave Craton: Composition, structure and origin. Journal of Petrology, **40**: 705–727. doi:10.1093/petrology/40.5.705.

Heise, W., and Pous, J. 2001. Effects of anisotropy on the two-dimensional inversion procedure. Geophysical Journal International, **147**: 610–621. doi:10.1046/j.0956-540x.2001.01560.x.

Helmstaedt, H.H., and Schultze, D.J. 1989. Southern African kimberlites and their mantle sample: implications for Archean tectonics and lithosphere evolution. *In* Kimberlites and related rocks, Vol. 1: Their composition, occurrence, origin, and emplacement. *Edited by* J. Ross. Geological Society of Australia, Special Publication 14, pp. 358–368.

Hood, C.T.S., and McCandless, T.E. 2004. Systematic variations in xenocryst mineral composition at the province scale, Buffalo Hills kimberlites, Alberta, Canada. Lithos, **77**: 733–747. doi:10.1016/j.lithos.2004.03.015.

Janse, A.J.A. 1994. Is Clifford's rule still valid? Affirmative examples from around the world. *In* Diamonds: characterization, genesis and exploration. Edited by H.O.A. Meyer and O.H. Leonardos. Companhia de Pesquisa de Recursos Minerais (CPRM) Special Publication, Brasilia, Brazil, pp. 215–235.

Jones, A.G. 1993. Electromagnetic images of modern and ancient subduction zones. Tectonophysics, **219**: 29–45. doi:10.1016/0040-1951(93)90285-R.

Jones, A.G., and Craven, J.A. 2004. Area selection for diamond exploration using deep probing electromagnetic surveying. Lithos, **77**: 765–782. doi:10.1016/j.lithos.2004.03.057.

Jones, A.G., and Gough, D.I. 1995. Electromagnetic images of crustal structures in southern and central Canadian Cordillera. Canadian Journal of Earth Sciences, **32**: 1541–1563.

Jones, A.G., and Spratt, J. 2002. A simple method for deriving the uniform field MT responses in auroral zones. Earth, Planets, and Space, **54**: 443–450.

Jones, A.G., Snyder, D., Hanmer, S., Asudeh, I., and White, D. 2002*a*. Magnetotelluric and teleseismic study across the Snowbird Tectonic Zone, Canadian Shield: a Neoarchean mantle suture? Geophysical Research Letters, **29**(17). doi:10.1029/2002GL015359.

Jones, F.W., Munro, R.A., Craven, J.A., Boerner, D.E., Kurtz, R.D., and Sydora, R.D. 2002*b*. Regional geoelectrical complexity of the Western Canada Basin from magnetotelluric tensor invariants. Earth, Planets, and Space, **54**: 899–905.

Jones, A.G., Lezaeta, P., Ferguson, I.J., Chave, A.D., Evans, R., Garcia, X., and Spratt, J. 2003. The electrical structure of the Slave craton. Lithos, **71**: 505–527. doi:10.1016/j.lithos.2003.08.001.

Jones, A.G., Ledo, J., and Ferguson, I. 2005. Electromagnetic images of the Trans-Hudson Orogen: the North American Central Plains anomaly revealed. Canadian Journal of Earth Sciences, **42**: 457–478. doi:10.1139/e05-018.

Jones, A.G., Garcia, X., Hamilton, M., Miensopust, M., Muller, M., Spratt, J., et al. and the SAMTEX team. 2006. SAMTEX (Southern African Magnetotelluric Experiment): overview and first results. *In*18th EM Induction Workshop, El Vendrell, Spain, 17–23 September.

Karato, S. 1990. The role of hydrogen in the electrical conductivity of the upper mantle. Nature, **347**: 272–273. doi:10.1038/347272a0.

Kirkley, M.B., Gurney, J.J., Otter, M.L., Hill, S.J., and Daniels, L.R. 1991. The application of C isotope measurements to the identification of the sources of C in diamonds: a review. Applied Geochemistry, **6**: 477–494. doi:10.1016/0883-2927(91)90048-T.

Kopylova, M.G., and Caro, G. 2004. Mantle xenoliths from the southeastern Slave craton: the evidence for a thick cold stratified lithosphere. Journal of Petrology, **45**: 1045–1067. doi:10.1093/petrology/egh003.

Luth, R. 1993. Diamonds, eclogites and the oxidation state of the Earth's mantle. Science, **261**: 66–69. doi:10.1126/science.261.5117.66.

McKenzie, D., and Priestley, K. 2008. The influence of lithospheric thickness variations on continental evolution. Lithos, **102**: 1–11. doi:10.1016/j.lithos.2007.05.005.

McNeice, G.M., and Jones, A.G. 2001. Multisite, multifrequency tensor decomposition of magnetotelluric data. Geophysics, **66**: 158–173. doi:10.1190/1.1444891.

Parkinson, W.D. 1959. Directions of rapid geomagnetic fluctuations. Geophysical Journal of the Royal Astronomical Society, **2**: 1–14.

Partzsch, G.M., Schilling, F.R., and Arndt, J. 2000. The influence of partial melting on the electrical behaviour of crustal rocks: laboratory examinations, model calculations and geological interpretations. Tectonophysics, **317**: 189–203. doi:10.1016/S0040-1951(99)00320-0.

Pilkington, M., Miles, W.F., Ross, G.M., and Roest, W.R. 2000. Potential-field signatures of buried Precambrian basement in the Western Canada Sedimentary Basin. Canadian Journal of Earth Sciences, **37**: 1453–1471. doi:10.1139/cjes-37-11-1453.

Power, M., Belcourt, G., and Rockel, E. 2004. Geophysical methods for kimberlite exploration in northern Canada. Leading Edge (Tulsa, Okla.), **23**: 1124–1129. doi:10.1190/1.1825939.

Rao, C.K., Jones, A.G., and Moorkamp, M. 2007. The geometry of the Iapetus suture in central Ireland deduced from a magnetotelluric survey. Geophysical Journal International, **161**: 134–141.

Rasmussen, T.M., Roberts, R.G., and Pedersen, L.B. 1987. Magnetotellurics along the Fennoscandian Long Range profile. Geophysical Journal International, **89**: 799–820. doi:10.1111/j.1365-246X.1987.tb05195.x.

Ritter, O., Hoffmann-Rothe, A., Bedrosian, P.A., Weckmann, U., and Haak, V. 2005. Electrical conductivity images of active and fossil fault zones. Geological Society (of London), Special Publications, 245, pp. 165–186.

Rodi, W., and Mackie, R.L. 2001. Nonlinear conjugate gradients algorithm for 2-D magnetotelluric inversion. Geophysics, **66**: 174–187. doi:10.1190/1.1444893.

Ross, G.M., and Eaton, D.W.S. 2002. Proterozoic tectonic accretion and growth of western Laurentia: results from Lithoprobe studies in northern Alberta. Canadian Journal of Earth Sciences, **39**: 313–329. doi:10.1139/e01-081.

Ross, G.M., Parrish, R.R., Villeneuve, M.E., and Bowring, S.A. 1991. Geophysics and geochronology of the crystalline basement of the Alberta Basin, western Canada. Canadian Journal of Earth Sciences, **28**: 512–522.

Ross, G.M., Mariano, J., and Dumont, R. 1994. Was Eocene magmatism widespread in the subsurface of southern Alberta? Evidence from new aeromagnetic data. Lithoprobe Alberta Basement Transect, **37**: 240–249.

Schilling, F.R., Partzsch, G.M., Brasse, H., and Schwarz, G. 1997. Partial melting below the magmatic arc in the central Andes deduced from geoelectromagnetic field experiments and laboratory data. Physics of the Earth and Planetary Interiors, **103**: 17–31. doi:10.1016/S0031-9201(97)00011-3.

Shragge, J., Bostock, M.G., Bank, C.G., and Ellis, R.M. 2002. Integrated teleseismic studies of the southern Alberta upper mantle. Canadian Journal of Earth Sciences, **39**: 399–411. doi:10.1139/e01-084.

Simpson, F., and Bahr, K. 2005. Practical Magnetotellurics. Cambridge University Press, New York, 270 p.

Siripunvaraporn, W., Egbert, G., Lenbury, Y., and Uyeshima, M. 2005. Three-dimensional magnetotelluric inversion: data-space method. Physics of the Earth and Planetary Interiors, **150**: 3–14. doi:10.1016/j.pepi.2004.08.023.

Skelton, D., Clements, B., McCandless, T.E., Hood, C., Aulbach, S., Davies, R., and Boyer, L.P. 2003. The Buffalo Head Hills

kimberlite province, Alberta. *In* Slave Province and northern Alberta field trip guidebook. Guidebook prepared for the 8th International Kimberlite Conference. *Edited by* B.A. Kjarsgaard. Victoria, pp. 11–20.

Soyer, W., and Unsworth, M.J. 2006. Deep electrical structure of the northern Cascadia subduction zone (British Columbia, Canada): implications for the role of fluids. Geology, **34**: 53–56. doi:10.1130/G21951.1.

Stachel, T., and Harris, J.W. 2008. The origin of cratonic diamonds—constraints from mineral inclusions. Ore Geology Reviews, **34**: 5–32. doi:10.1016/j.oregeorev.2007.05.002.

Stachel, T., Harris, J.W., Tappert, R., and Brey, G.P. 2003. Peridotitic diamonds from the Slave and the Kaapvaal cratons—similarities and differences based on a preliminary data set. Lithos, **71**: 489–503. doi:10.1016/S0024-4937(03)00127-0.

Swift, C.M. 1967. A magnetotelluric investigation of electrical conductivity anomaly in the southwestern United States. Ph.D. thesis, Massachusetts Institute of Technology *Edited by* K. Vozoff. Geophysics Reprint Series no. 5, pp.156–166). (Reprinted in Magnetotelluric Methods. 1988.)

Tappert, R., Stachel, T., Harris, J.W., Muehlenbachs, K., Ludwig, T., and Brey, G.P. 2005. Subducting oceanic crust: the source of deep diamonds. Geology, **33**: 565–568. doi:10.1130/G21637.1.

Tauber, S., Banks, R., Ritter, O., and Weckmann, U. 2003. A high-resolution magnetotelluric survey of the Iapetus Suture Zone in southwest Scotland. Geophysical Journal International, **153**: 548–568. doi:10.1046/j.1365-246X.2003.01912.x.

Thériault, R.J., and Ross, G.M. 1991. Nd isotopic evidence for crustal recycling in the ca. 2.9 Ga subsurface of western Canada. Canadian Journal of Earth Sciences, **28**: 1140–1147.

Villeneuve, M.E., Ross, G.M., Parrish, R.R., Thériault, R.J., Miles, W., and Broome, J. 1993. Geophysical subdivision, U–Pb geochronology and Sm–Nd isotope geochemistry of the crystalline basement of the Western Canada Sedimentary Basin, Alberta and northeastern British Columbia. Geological Survey of Canada, Bulletin 447, 86 p.

Vozoff, K. 1991. The magnetotelluric method. *In* Electromagnetic methods in applied geophysics. *Edited by* M.N. Nabighian. Society of Exploration Geophysicists, Tulsa, Okla., pp. 641–711.

Wiese, H. 1962. Geomagnetische Tiefentellurik Teil II: Die Streichrichtung der Untergrundstrukturen des elektrischen Widerstandes, erschlossen aus geomagnetischen Variationen. Pure and Applied Geophysics, **52**: 83–103.

Wu, X., Ferguson, I.J., and Jones, A.G. 2005. Geoelectric structure of the Proterozoic Wopmay Orogen and adjacent terranes, Northwest Territories, Canada. Canadian Journal of Earth Sciences, **42**: 955–981. doi:10.1139/e05-042.

Wyllie, P.J., and Huang, W.-L. 1976. Carbonation and melting reactions in the system CaO–MgO–SiO_2–CO_2 at mantle pressures with geophysical and petrological applications. Contributions to Mineralogy and Petrology, **54**: 79–107. doi:10.1007/BF00372117.

Xu, Y., Shankland, T.J., and Poe, B.T. 2000. Laboratory-based electrical conductivity of the Earth's mantle. Journal of Geophysical Research, **105**: 27 865 – 27 875. doi:10.1029/2000JB900299.

Appendix A. Two-dimensional magnetotelluric inversions

The two-dimensional (2-D) inversion algorithm of Rodi and Mackie (2001) was used to invert individual profiles of magnetotelluric (MT) data and uses several parameters to control the smoothness of the resistivity model. The parameter tau (τ) controls the trade-off between the degree of smoothing and fit to the measured MT data. The parameter alpha (α) controls the vertical to horizontal smoothing of the model. The quality of the fit to the measured MT data is quantified by the root mean square (rms) misfit, which should ideally have the value 1. In practice a value in the range 1–1.5 is acceptable, provided that a range of tau (τ) values are used to ensure the model has the correct balance of misfit and smoothness. A joint inversion of the transverse electric (TE) and transverse magnetic (TM) mode data is generally required since each mode is sensitive to different aspects of the geoelectric structure (Berdichevsky et al. 1998). Many individual inversions of each profile were performed with a wide range of τ and α values. Varying τ from 0.1 to 100 produced a set of models with improved smoothness and worse rms misfit. A value of τ = 10 was chosen as a compromise between these competing goals and inversions with α = 3 are shown in Fig. 7. The parameter α determines the degree to which the model is smoothed in the horizontal and vertical directions. The rms misfits for the NAB profile

Fig. A1. Apparent resistivity and phase curves representing general characteristics of observed data at northern end of NAB profile. Data are displayed in a N37°E coordinate system. Black line shows the fit of the 2-D inversion (Fig. 7) and the grey line shows the fit of the 3-D inversion.

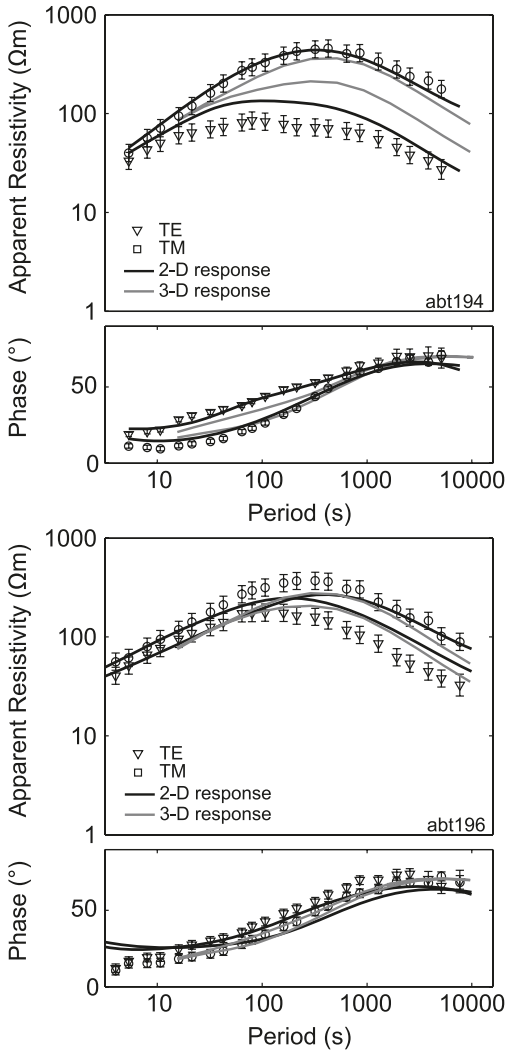

Fig. A2. (*a*) The 2-D inversion of field data on the NAB and A profiles. (*b*) The 2-D inversion of synthetic data obtained from the 3-D inversion model in (*c*). Note that the conductor located at the intersection of the profiles in (*b*) is partially an artifact. (*c*) Depiction of 2-D slices of the 3-D resistivity model. Note that station geometry used in the 2-D inversions was obtained by projecting the stations onto a line perpendicular to the strike direction. Therefore, the section views of 2-D inversions (*a*–*b*) are shorter than the actual profile lengths shown on the maps and 3-D model (*c*).

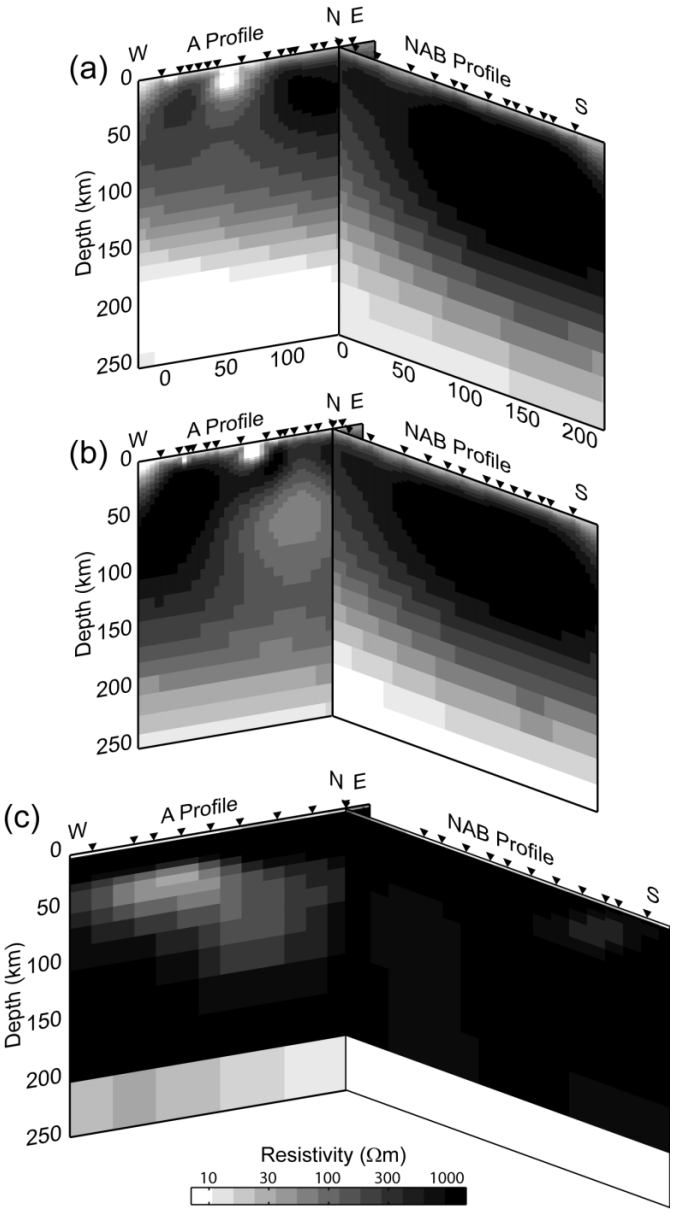

inversions for the TE and TM data are 1.37–1.46, values which are both acceptable. The fit of the 2-D NAB inversion to the measured data is shown in Fig. 6*b*, and it can be seen that the data are well fit across the entire period range.

The vertical magnetic transfer functions (tipper) data can also be included in the inversion and are useful because they are more sensitive than the apparent resistivity and phase to horizontal changes in resistivity. However, the tipper data must only be included if they can be considered 2-D, i.e., the tipper is consistent with the TE and TM mode apparent resistivity – phase data. The TE, TM, and tipper inversion for the A profile has a relatively high rms misfit value (2.48) that may indicate the inversion is not capable of simultaneously fitting the three subsets of the data. It was previously shown that the magnitude and orientation of the long-period induction vectors suggest that non-uniform source effects are present in the data. Thus the interpretation in this paper is focused on models derived from just TE and TM mode data. In all inversions, static shifts were estimated by the inversion algorithm. These values were generally small and in the range 2–0.5. The 2-D inversion shows an upper mantle conductor at the north end of the NAB profile. This is due to lower apparent resistivity values, as can be seen in the pseudosection in Fig. 6. The fit to observed data is shown in Fig. 5 and Fig. A1.

A three-dimensional (3-D) inversion was used to determine whether the 2-D inversions were valid. The 2-D and 3-D inversion models were quite different, which suggests the 2-D inversion models contain artifacts. To investigate this effect, a simple test was undertaken. The 3-D model was used to generate synthetic MT data at the same periods as the field MT data. The synthetic 3-D MT data were then rotated to N37°E and inverted using the same 2-D inversion approach as for the actual MT data. The resulting 2-D model is shown in Fig. A2. This 2-D inversion shows an upper mantle conductive zone at the northern end of NAB profile that was not in the original 3-D model in Fig. A2 and was caused by stations at the north end of the NAB profile. This strongly suggests that the conductor imaged at the northern end of the NAB profile in the 2-D inversion is an artifact and not required by the MT data. This is despite strong indications that the data can be considered 2-D (strike direction, skew, etc.).